EXPERIMENTAL INVESTIGATION AND MATHEMATICAL MODELING OF THE CONCRETE CARBONATION PROBLEM

VAGELIS G. PAPADAKIS and COSTAS G. VAYENAS[†]
Institute of Chemical Engineering and High Temperature Chemical Processes and Department of
Chemical Engineering, University of Patras, Patras GR 26110, Greece

and

MICHAEL N. FARDIS
Department of Civil Engineering, University of Patras, Patras GR 26110, Greece

Abstract—Carbonation of concrete is the major time-limiting factor for the durability of reinforced concrete structures. The carbonation reaction between atmospheric CO_2 and $Ca(OH)_2$ of the concrete mass destroys the high pH environment of surrounding concrete which protects the steel bars of reinforced concrete from corrosion. In this paper we present experimental results obtained in an accelerated carbonation apparatus using a variety of techniques, including TGA, and we extend the mathematical model developed recently to include the entire range of ambient relative humidities.

1. INTRODUCTION

Concrete is the most widely used construction material, not only because of its low cost, but also due to its high durability. However, in the last two decades the instances of unsatisfactory durability of concrete structures have increased at an alarming rate. In most cases this is due to corrosion of the reinforcing steel in reinforced concrete. Corrosion reduces the available cross-sectional area of a reinforcing steel bar and hence its strength. It also introduces a bursting internal pressure on the surrounding concrete, since the volume of the corrosion products is much higher than that of the corroding metal. As a result of this serious problem, a significant research effort has begun in recent years aiming at the development of a thorough understanding of the mechanisms leading to reinforcement corrosion and of effective measures to control it.

Reinforcing steel bars in concrete are protected from corrosion by a thin oxide layer that forms on their surface due to the highly alkaline environment of the surrounding concrete (pH around 13). This alkalinity is due to $Ca(OH)_2$ produced during the reaction between water and the constituents of cement which causes the hardening and development of strength of cement and concrete. The chemistry of these hydration reactions have been reviewed througly (Brunauer and Copeland, 1964; Bensted, 1983; Frigione, 1983; Taylor, 1986).

Corrosion of the reinforcing steel bars may start when the protective oxide layer is destroyed, either by chloride penetration or due to a reduction in the pH value of concrete to values below 9. Such a decrease in alkalinity is the result of carbonation of $Ca(OH)_2$ in the concrete mass, i.e., of the reaction between $Ca(OH)_2$ and atmospheric CO_2 which diffuses through the pores of concrete. In marine and coastal environments, or in the presence of deicing salts, chloride penetration is the main mechanism causing reinforcement corrosion. In all other cases, and particularly in CO_2-rich urban environments, carbonation of concrete is the main mechanism leading to steel corrosion.

The problem of reinforcement depassivation by chloride ions has been studied thoroughly by Pereira and Hegedus (1984). These authors were the first to recognize that the phenomenon can be treated as a classical reaction engineering problem. Their quantitative chloride ion diffusion–reaction model was found to be in very good agreement with experiment.

There have been several experimental studies of concrete carbonation both for outdoor conditions (Schiessl, 1976; Nagataki *et al.*, 1986) and for controlled indoor conditions (Tuutti, 1982; Nagataki *et al.*, 1986, 1988; Ying-yu and Qui-dong, 1987). These studies showed that a "carbonation front" is created, the location of which proceeds proportionally with $\sqrt{t}$, i.e.:

$$x_c = A\sqrt{t}. \tag{1}$$

In a recent study (Papadakis *et al.*, 1989) a reaction engineering model was developed, starting from first principles, to explain the semiempirical eq. (1). It was shown that, in the limit of a CO_2 diffusion controlled carbonation process, eq. (1) is valid in the form:

$$x_c = [2[CO_2]^0 D_{e,CO_2}/([Ca(OH)_2]^0 + [CSH]^0)]^{1/2} \sqrt{t} \tag{2}$$

[†]Author to whom correspondence should be addressed.

where $[CO_2]^0$ is the ambient CO_2 concentration, D_{e,CO_2} is the effective diffusivity of CO_2 in concrete and $[Ca(OH)_2]^0$ and $[CSH]^0$ are the concentrations of $Ca(OH)_2$ and $3CaO \cdot 2SiO_2 \cdot 3H_2O$ (CSH = calcium silicate hydrate) at the end of the hydration period. Equation (2) was found to provide a good fit to experimental data for relative humidity values (RH) above 50%. For lower RH values significant deviations were observed.

The objectives of this work are:

1. To examine experimentally the conditions over which a "carbonation front" is indeed formed, by the use of thermogravimetric analysis (TGA);

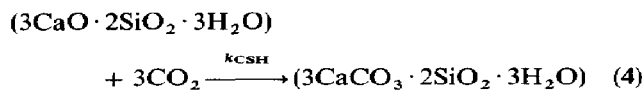2. To study the effect of relative humidity on D_{e,CO_2};

3. To study the evolution of the carbonation process for RH values both above and below 50% and to examine if the reaction engineering model of Papadakis et al. (1989) can adequately describe the process over the entire RH range.

2. PHYSICOCHEMICAL CONSIDERATIONS

The carbonation of concrete takes place in the cement paste component of concrete, whereas aggregates, which constitute the major part of the mass and volume of concrete, are essentially inert fillers, as far as carbonation is concerned. However, aggregates affect several parameters, and thus all model quantities described below refer to the total mass of concrete.

Cement paste is the product of the hydration reactions of the constituents of cement. The main constituents are $3CaO \cdot SiO_2$ (C_3S = tricalcium silicate), $2CaO \cdot SiO_2$ (C_2S = dicalcium silicate), and in lesser amounts, $4CaO \cdot Al_2O_3 \cdot Fe_2O_3$ (C_4AF = calcium aluminoferrite), $3CaO \cdot Al_2O_3$ (C_3A = tricalcium aluminate) and $CaSO_4 \cdot 2H_2O$ (gypsum). The hydration reactions have characteristic time constants of the order of 20 days (Brunauer and Copeland, 1964; Taylor, 1986; Papadakis et al., 1989) and approach 90% completion usually 3 months after casting of concrete. Their chemistry has been reviewed thoroughly (Brunauer and Copeland, 1964; Bensted, 1983; Frigione, 1983; Taylor, 1986) and has recently been presented in a summarized form (Papadakis et al., 1991a). The hydration reactions produce $Ca(OH)_2$ and the main strength element of hardened cement paste, i.e., $3CaO \cdot 2SiO_2 \cdot 3H_2O$ (CSH = calcium silicate hydrate). These hydration products, both susceptible to carbonation, constitute typically 25% wt and 60% wt of the mass of hardened cement paste, respectively. Other hydration products containing complex CaO, Al_2O_3, Fe_2O_3 and $CaSO_4$ compounds are also formed (Papadakis et al., 1991a) but, since they constitute typically less than 15% wt of the mass of hardened cement paste and since they are susceptible only to surface and not bulk carbonation (Bensted, 1983), they are not considered here.

Consequently the carbonation reactions which must be taken into account are:

$$Ca(OH)_2 + CO_2 \xrightarrow{k_{CH}} CaCO_3 + H_2O \qquad (3)$$

$$(3CaO \cdot 2SiO_2 \cdot 3H_2O)$$
$$+ 3CO_2 \xrightarrow{k_{CSH}} (3CaCO_3 \cdot 2SiO_2 \cdot 3H_2O) \qquad (4)$$

where the symbols CH and CSH denote $Ca(OH)_2$ and calcium silicate hydrate, respectively.

Water, which is always present in larger or lesser amounts in the pores of hardened cement paste, plays a key role in the process of carbonation. Its role is two-fold: first it blocks pores and thus hinders diffusion of CO_2; second it provides a medium for reactions (3) and (4). This is why, as shown below, the carbonation depth goes through a maximum with increasing relative humidity or, equivalently, with increasing amount of water in the concrete pores.

3. EXPERIMENTAL PROCEDURES

Concrete samples were prepared using ordinary Portland cement (OPC) of normal fineness (Type-I cement), weight water to cement ratio ($R_{w/c}$) equal to 0.65 and weight aggregate to cement ratio ($R_{a/c}$) equal to 3 and 5. Experimental details can be found elsewhere (Papadakis et al., 1991b). Two sample geometries were used: cylindrical pellets (26 mm diameter, 10 mm thickness) for D_{e,CO_2} measurements and slabs (100 mm $\times$ 100 mm $\times$ 300 mm) for the accelerated carbonation and TGA measurements. After molding in appropriate plexiglass molds for 24 h, the molds were stripped and the samples were placed under water at 30°C for 90 days in order for the hydration reactions to reach completion prior to exposure to carbonation. Special precautions were taken to avoid diffusion of $Ca(OH)_2$ produced during hydration out of the samples, by adding enough $Ca(OH)_2$ to the curing water to achieve a saturated solution.

3.1. Effective diffusivity measurements

A Wicke–Kallenbach apparatus described elsewhere (Papadakis et al., 1991a) was used to measure effective diffusivities both in uncarbonated and carbonated samples. In the former case, in order to overcome the problem of CO_2 reaction with concrete constituents, D_{e,N_2} was measured and D_{e,CO_2} was computed from

$$D_{e,CO_2} = \sqrt{M_{N_2}/M_{CO_2}} \cdot D_{e,N_2} = 0.8 D_{e,N_2}. \qquad (5)$$

Equation (5) is exactly valid only if Knudsen diffusion prevails. This is a good approximation as verified both from D_e measurements in carbonated samples and from the concrete pore-size distribution (Papadakis et al., 1989, 1991a).

3.2. Thermogravimetric analysis (TGA)

Concrete samples exposed to accelerated carbonation conditions for 10 days were cut into 5 mm thickness slices parallel to the CO_2-exposed surface. A TGA apparatus (Dupont Model 990 at 10°C/min in

N_2) was used to measure quantitatively the solid concentrations of $Ca(OH)_2$ and $CaCO_3$ in the slices and thus to obtain the corresponding concentration profiles.

3.3. Accelerated carbonation apparatus

Because in normal environments, which contain 0.03–0.05% CO_2, the evolution of carbonation depth with time is very slow and, typically, samples are studied over periods of 5–10 years (Nagataki et al., 1986; Litvan and Meyer, 1986), an accelerated carbonation chamber was used where concrete samples were exposed to 50% CO_2–50% air mixtures under controlled temperature and RH conditions. The chamber is described in detail elsewhere (Papadakis et al., 1991b). Its use leads to a dramatic reduction in the time needed to perform the experiments. Thus it can be seen from eq. (2) that in order to obtain the same carbonation depth, e.g. 1 cm, the ratio t_1/t_2 of time t_1 required under normal exposure conditions and of the time t_2 under accelerated test conditions is $p_{CO_2,2}/p_{CO_2,1}$, i.e. $\simeq 10^3$. Thus one can study in the chamber within a few days what would happen under normal exposure conditions in many years.

The accelerated carbonation tests were interrupted six times, after the samples had been exposed to the CO_2-rich chamber atmosphere for 1, 3, 5, 10, 15 and 20 days, respectively. At each interruption two 20-mm-thick slices were cut normal to the long dimension of the sample, one from each end of the sample. The shortened sample was put back into the chamber and its exposure to the 50% CO_2–50% air mixture was continued. The fresh cut surface of each slice was cleaned and sprayed with a phenolphthalein pH-indicator. The average carbonation depth was measured normal to both sides of each slice, immediately after spraying and after 24 h. The average of all eight measurements was taken as the carbonation depth at the time of the test interruption. Even when no sharp carbonation front is formed, i.e., for low RH values as discussed below, the phenolphthalein indicator, which changes color at pH 9.3, shows the location where the concentration of $Ca(OH)_2$ has practically vanished.

4. RESULTS AND DISCUSSION

4.1. Effective diffusivity

Figure 1 shows the effect of RH on D_{e,CO_2}. Increasing RH causes an increase in the volume fraction f of pores occupied by H_2O, both by filling the pores with radii below the corresponding Kelvin radius and by increasing the thickness of the aqueous film on the walls of larger pores (Papadakis et al., 1989, 1991a). Consequently, D_{e,CO_2} decreases substantially with increasing RH. It was found that the data can be fitted well by the following empirical expression:

$$\sqrt{D_e} = B\epsilon_p[1 - (RH/100)] \qquad (6)$$

where ϵ_p is the cement paste porosity and $B = (1.2 \pm 0.1)\ 10^{-3}\ m/s^{1/2}$. Figure 1 also shows that carbonation causes a small decrease in D_{e,CO_2}. This is due

to the reduction in porosity and mean pore radius as evidenced by BET and mercury porosimetry (Papadakis et al., 1991a).

4.2. TGA concentration profiles

Figure 2 shows typical TGA results obtained with two identical concrete samples exposed to 50% CO_2 for 10 days, one at $RH = 65\%$, the other at $RH = 37\%$. In the former case $Ca(OH)_2$ and $CaCO_3$ do not coexist in any sample location, but in the latter they do exist over a rather wide distance. The concentrations of $Ca(OH)_2$ and $CaCO_3$, computed from the TGA results of Fig. 2 by means of the procedure proposed by Taylor et al. (1985), are compared in Fig. 3 with those predicted by eq. (2) and also by the mathematical model discussed below. The results for $RH = 65\%$ [Fig. 3(a)] are consistent with the formation of a sharp carbonation front, but the results for $RH = 37\%$ [Fig. 3(b)] are not. This turns out to be consistent with the carbonation depth experiments and can be explained within the framework of the mathematical model discussed below. The curves in Fig. 3 result from this model.
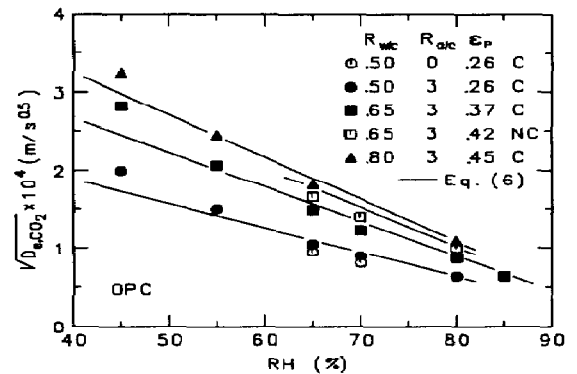

Fig. 1. Effect of ambient relative humidity (RH) on the effective diffusivity of CO_2 in concrete. C: carbonated; NC: non-carbonated.
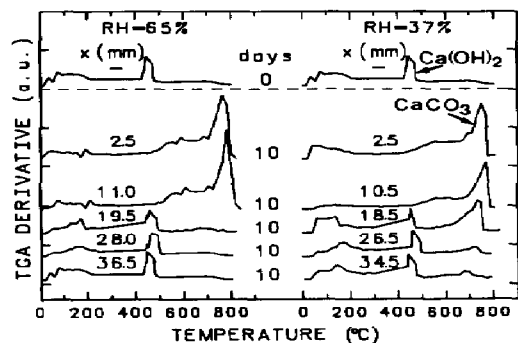

Fig. 2. Derivatives of thermogravimetric analysis curves of sections of OPC concrete ($R_{w/c} = 0.65$, $R_{a/c} = 3$) exposed to 50% CO_2 at $RH = 65\%$ (left) and $RH = 37\%$ (right)
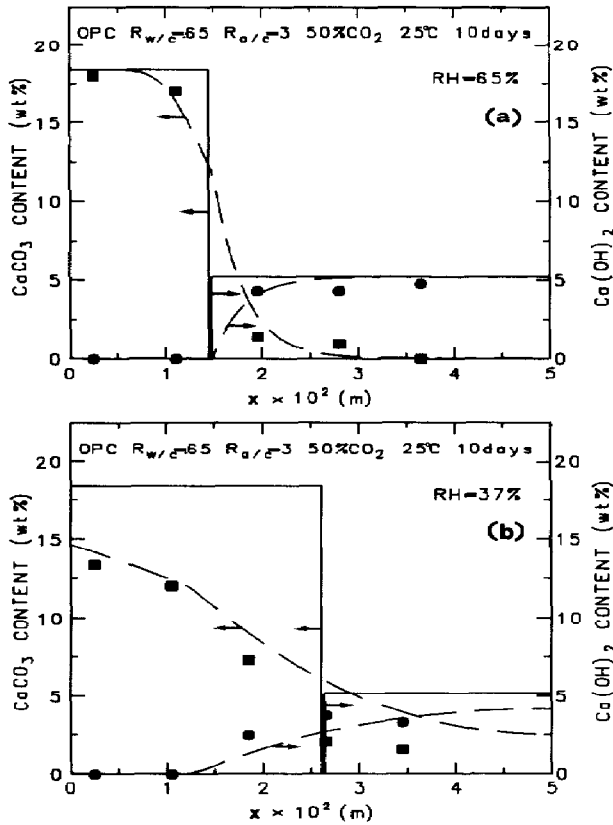
Fig. 3. Effect of distance x from CO_2 exposed concrete surface on the concentration of $Ca(OH)_2$ and $CaCO_3$. Solid lines from eq. (2); dashed lines from numerical solution. Circles: $Ca(OH)_2$ content; squares: $CaCO_3$ content, both obtained by TGA.

Fig. 4. Dependence of carbonation depth (x_c) on $t' = ty^0_{CO_2}$ at 65% RH. Open symbols: $y^0_{CO_2} = 0.005$; filled symbols: $y^0_{CO_2} = 0.5$; atmospheric total pressure.

Fig. 5. Effect of RH on carbonation depth. Solid line from eq. (2). Dashed curves from numerical simulation for various n values in eq. (14).

4.3. *Carbonation depth measurements*

Figure 4 shows carbonation depth results obtained both in this work and by previous workers (Nagataki *et al.*, 1986). Open symbols are data obtained under normal CO_2 exposure conditions over a period of years. Filled symbols are data obtained under accelerated carbonation conditions over a period of several days. By using a new time scale $t' = y^0_{CO_2} \cdot t$, where $y^0_{CO_2}$ is the mole fraction of CO_2, all results fall on the same line. The solid straight line in the figure corresponds to eq. (2) with D_{e,CO_2} measured independently in the Wicke–Kallenbach apparatus. There is excellent agreement between experiment and theory (Papadakis *et al.*, 1989). However, it must be noted that all results shown in Fig. 4 have been obtained at constant $RH = 65\%$, i.e., under conditions where a sharp carbonation front is formed [Fig. 3(a)]. It is only under such conditions that the rate is entirely controlled by CO_2 diffusion and, consequently, eq. (2) is valid.

Figure 5 shows the effect of RH on carbonation depth. The solid straight line corresponds to eqs (2) and (6) with D_{e,CO_2} again measured in the Wicke–Kallenbach apparatus. It is worth noting that
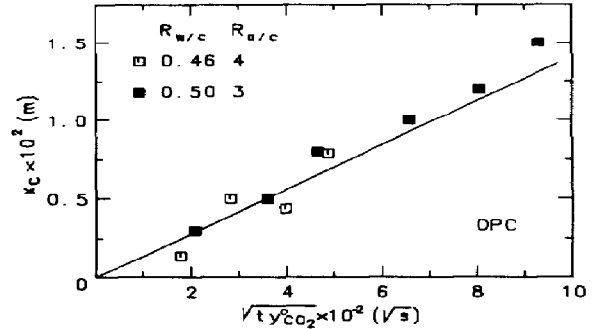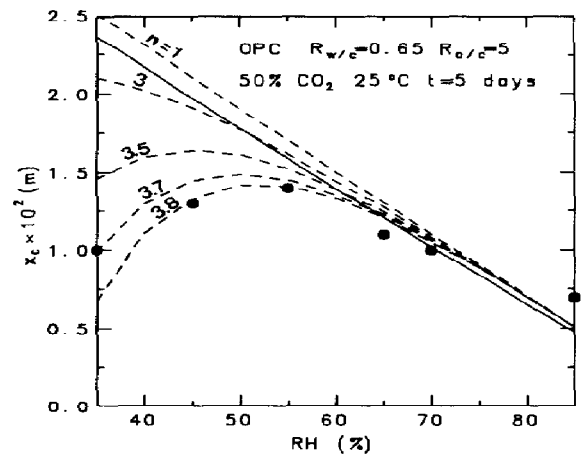
because x_c is proportional to $\sqrt{D_{e,CO_2}}$ [eq. (2)] and $\sqrt{D_{e,CO_2}}$ decreases linearly with RH [Fig. 1 and eq. (6)], x_c is predicted to decrease linearly with RH. The experimental results in Fig. 5 show that this is indeed the case for $RH > 50\%$. Lower RH values lead to significant deviations as x_c goes through a maximum and eq. (2) is clearly no longer valid.

The physical reason for the deviations for $RH < 50\%$ is the following: eq. (2) holds only to the extent that CO_2 diffusion is rate limiting, i.e., only when reactions (3) and (4) are very fast relative to CO_2 diffusion. As RH decreases, the water content in the pores decreases and thus reactions (3) and (4), which take place in the aqueous phase (Papadakis *et al.*, 1989), become slow and start controlling the carbonation rate. The latter becomes significantly smaller than its diffusion-controlled limit represented by eq. (2) and by the solid straight line in Fig. 5.

4.4. *Mathematical modeling*

In a recent paper (Papadakis et al., 1989), a detailed mathematical model was developed to describe concrete carbonation with simultaneous occurrence of the hydration reactions. This model examines a slab geometry and has been solved only for the limiting case of very fast carbonation kinetics leading to the limiting analytical eq. (2), which is in good agreement with experiment for $RH > 50\%$. In the following we examine whether this model, when solved numerically, can describe the observed behavior over the entire RH range. Since the experiments were conducted with fully hydrated samples, we present here only the simplified model equations (in dimensionless form) when all hydration reaction rates are set to zero. Also the pseudo-steady-state approximation has been used (Wen, 1968; Froment and Bischoff, 1979) and the terms describing dissolved $Ca(OH)_2$ diffusion in the aqueous phase have been omitted in good approximation, as explained elsewhere (Papadakis et al., 1989).

Denoting by C, C_{CH} and C_{CSH} the dimensionless concentrations of CO_2, $Ca(OH)_2$ and CSH, respectively, one has the following simplified dimensionless differential mass balances of CO_2, $Ca(OH)_2$ and CSH:

$$0 = \frac{\partial}{\partial z}\left(\delta\frac{\partial C}{\partial z}\right) - \Phi^2 C\left[C_{CH} + 3\alpha_{CHS}C_{CSH}\right] \quad (7)$$

$$\beta\frac{\partial(C_{CH})}{\partial\tau} = -\Phi^2 C C_{CH} \quad (8)$$

$$\beta_{CSH}\frac{\partial(C_{CSH})}{\partial\tau} = -\Phi^2\alpha_{CSH}C C_{CSH} \quad (9)$$

where the parameters δ, Φ^2, α_{CSH}, β, β_{CSH} and the dimensionless time τ are defined in the Notation section. The initial and boundary conditions are:

at $\tau = 0$: $C_{CH} = C_{CSH} = 1$ (10a)

at the concrete outer surface, $z = 0$: $C = 1$ (10b)

at the symmetry axis, $z = 1$: $\partial C/\partial z = 0$.   (10c)

It is worth noting that when Φ^2 is large, i.e., of the order of 10^5 as it is for $RH > 50\%$ (Papadakis et al., 1989), then eqs (7)–(10) reduce to:

$$C = 1 - z/z_c, \quad C_{CH} = C_{CSH} = 0 \quad \text{for } 0 \leqslant z \leqslant z_c$$
$$(11)$$

$$C = 0, \quad C_{CH} = C_{CSH} = 1 \quad \text{for } z_c < z < 1 \quad (12)$$

with $z_c = [2\delta_c\tau/(\beta + 3\beta_{CSH})]^{1/2}$.   (13)

Equation (13) is the dimensionless form of eq. (2), i.e., the model predicts a sharp carbonation front.

However, when Φ^2 is finite, eqs (7)–(10) must be solved numerically. This was done using the finite difference method with Euler integration in time. The model contains, *a priori*, no adjustable parameters, since all the quantities appearing in eqs (7)–(9) are independently measurable and since literature values are used for the kinetic constant k_{CH} of reaction (3) (Danckwerts, 1970; Papadakis et al., 1989). There is only some uncertainty about the ratio of kinetic

constants of reactions (4) and (3), k_{CSH}/k_{CH}, for which only a lower estimate (2.4×10^{-3}) can be obtained from the literature (Sauman, 1971). By fitting the model to the TGA data (Fig. 3) a better estimate was obtained (7.8×10^{-3}) and this was used in the numerical simulations. It was then found that the model could not provide a satisfactory fit to the low RH data (Fig. 5, curve labeled $n = 1$) as it predicts a maximum in x_c at very low RH values ($\simeq 10\%$). It was then decided to examine whether the model can describe the x_c vs RH data by considering that k_{CH} is a function of f. This is reasonable in view of the fact that the literature k_{CH} values (Danckwerts, 1970) have been measured in bulk aqueous solutions with dimensions orders of magnitude larger than molecular dimensions. This is not the case in concrete pores where the dimensions of micropores are of the order of a few angstroms (Papadakis et al., 1989, 1991a) and the aqueous film thickness on the walls of larger pores is typically 1–3 molecular dimensions and decreases with decreasing RH and f. In such aqueous environments mass transport of ions (e.g. OH^-, HCO_3^-) which, to a large extent, controls the rate of reaction (3) (Danckwerts, 1970), must follow different molecular mechanisms and obey different transport expressions than in bulk aqueous media, particularly when one takes into account the strong ion–pore wall molecular interactions. It was thus found that all the data (Figs 1, 3 and 5) can be fitted adequately by setting:

$$k_{CH} = k_{CH}^0 f^n \quad (14)$$

where $n = 3.7$ (Fig. 5) and k_{CH}^0 is the kinetic constant value in a bulk aqueous solution. Despite the empirical nature of eq. (14) there is, as mentioned above, good physicochemical reason to expect that k_{CH} will vary with aqueous film thickness and thus with f.

5. CONCLUDING REMARKS

Concrete carbonation, which is the major time limiting factor for the durability of reinforced concrete structures, can be studied and modeled using standard reaction engineering tools. Both the TGA and the carbonation depth results show that a sharp carbonation front is indeed formed for relative humidities above 50%. Under such conditions the evolution in time of the carbonation front is given by the simple analytical expression (2). At lower RH values no sharp front is formed and the kinetics of the carbonation reactions become important. Comparison of the experimental results with the detailed reaction engineering model developed recently (Papadakis et al., 1989) to describe concrete hydration and carbonation provides strong indication that the kinetics of the carbonation reactions are affected by the aqueous film thickness when the latter reaches molecular dimensions. When this is taken into account the model is in good agreement with experiment.

NOTATION

A proportionality constant in eq. (1), $m/s^{1/2}$

C	dimensionless concentration of CO_2
C_{CH}	dimensionless concentration of $Ca(OH)_2$
C_{CSH}	dimensionless concentration of CSH
$[Ca(OH)_2]$	molar concentration of $Ca(OH)_2$, mol/m^3
$[CO_2]$	molar concentration of CO_2, mol/m^3
$[CSH]$	molar concentration of CSH, mol/m^3
D_{e,CO_2}	effective diffusivity of CO_2, m^2/s
D_{e,N_2}	effective diffusivity of N_2, m^2/s
f	total fraction of pore volume filled with water
k_{CH}, k_{CSH}	carbonation rate constants of $Ca(OH)_2$ and CSH, $m^3/mol \cdot s$
L	distance between outer surface and axis of symmetry, m
M	molecular weight
n	parameter defined in eq. (14)
$R_{a/c}$	aggregate to cement ratio by weight
$R_{w/c}$	water to cement ratio by weight
RH	relative humidity of gas phase, %
t, t'	time and generalized time, respectively, s
x	distance from the outer surface of concrete, m
x_c	carbonation depth, m
y_{CO_2}	molar fraction of CO_2
z	dimensionless distance
z_c	dimensionless carbonation depth

Greek letters

α_{CSH}	$k_{CSH}[CSH]^0/k_{CH}[Ca(OH)_2]^0$
β, β_{CSH}	$[Ca(OH)_2]^0/\epsilon^0(1-f)[CO_2]^0$, $[CSH]^0/\epsilon^0(1-f)[CO_2]^0$, respectively
δ	dimensionless effective diffusivity of CO_2, $D_{e,CO_2}/D^0_{e,CO_2}$
ϵ, ϵ_p	concrete and cement paste porosity, respectively
τ	dimensionless time, $D^0_{e,CO_2}t/[\epsilon^0(1-f)L^2]$
Φ	Thiele modulus, $(L^2 k_{CH}[Ca(OH)_2]^0/D^0_{e,CO_2})^{1/2}$

Subscript

c	quantities referring to carbonated area

Superscript

0	quantities referring to initial conditions $(t = 0)$

REFERENCES

Bensted, J., 1983, Hydration of Portland cement. In *Advances in Cement Technology* (Edited by Ghosh, S. N.), pp. 307–347. Pergamon Press, New York.

Brunauer, S. and Copeland, L. E., 1964, The chemistry of concrete. *Scient. Am.* 210, 80–92.

Danckwerts, P. V., 1970, *Gas–Liquid Reactions.* McGraw-Hill, New York.

Frigione, G., 1983, Gypsum in cement. In *Advances in Cement Technology* (Edited by Ghosh, S. N.), pp. 485–535. Pergamon Press, New York.

Froment, G. F. and Bischoff, K. B., 1979, *Chemical Reactor Analysis and Design.* John Wiley, New York.

Litvan, G. G. and Meyer, A., 1986 Carbonation of granulated blast furnace slag cement concrete during twenty years of field exposure. In *Proc. 2nd Int. Conf. on the Use of Fly Ash, Silica Fume, Slag and Natural Pozzolans in Concrete*, ACI, SP 91, pp. 1445–1462, Madrid.

Nagataki, S., Ohga, H. and Kim, E. K., 1986, Effects of curing conditions on the carbonation of concrete with fly ash and the corrosion of reinforcement in long-term tests. In *Proc. 2nd Int. Conf. on the Use of Fly Ash, Silica Fume, Slag and Natural Pozzolans in Concrete*, ACI, SP 91, pp. 521–539, Madrid.

Nagataki, S., Mansur, M. A. and Ohga, H., 1988, Carbonation of mortar in relation to ferrocement construction. *Am. Concr. Inst. Mater. J.* 85, 17–25.

Papadakis, V. G., Vayenas, C. G. and Fardis, M. N., 1989, A reaction engineering approach to the problem of concrete carbonation. *A.I.Ch.E. J.* 35, 1639–1650.

Papadakis, V. G., Vayenas, C. G. and Fardis, M. N., 1991a, Physical and chemical characteristics affecting the durability of concrete. *Am. Concr. Inst. Mater. J.* (in press).

Papadakis, V. G., Vayenas, C. G. and Fardis, M. N., 1991b, Fundamental modeling and experimental investigation of concrete carbonation. *Am. Concr. Inst. Mater. J.* (in press).

Pereira, C. J. and Hegedus, L. L., 1984, Diffusion and reaction of chloride ions in porous concrete. In *Proc. 8th Int. Symp. of Chemical Reaction Engineering*, Edinburgh.

Sauman, Z., 1971, Carbonization of porous concrete and its main binding components. *Cem. Concr. Res.* 1, 645–662.

Schiessl, P., 1976, Zur Frage der Zulässigen Rissbreite und der Erfoderlichen Betondeckung im Stahlbetonbau unter Besonderer Berücksichtigung der Karbonatisierung des Betons. *Deutscher Ausschuss für Stahlbeton* 255.

Taylor, H. F. W., 1986, Chemistry of cement hydration. In *Proc. 8th Int. Congress on the Chemistry of Cement*, pp. 82–110.

Taylor, H. F. W., Mohan, K. and Moir, G. K., 1985, Analytical study of pure and extended Portland cement pastes: I. Pure Portland cement pastes. *J. Am. Ceram. Soc.* 68, 680–685.

Tuutti, K., 1982, *Corrosion of Steel in Concrete.* CBI Forskning Research, Swedish Cement and Concrete Research Institute, Stockholm.

Wen, G. Y., 1968, Noncatalytic heterogeneous solid fluid reaction models. *Ind. Engng Chem.* 60, 34–54.

Ying-yu, L. and Qui-dong, W., 1987, The mechanism of carbonation of mortar and the dependence of carbonation on pore structure. In *Proc. Katharine and Bryant Mather Int. Conf. on Concrete Durability*, ACI, SP 100, pp. 1915–1943, Atlanta.